第 27卷 第 1期 焊 接 学 报 Vol 27 No. 1
2006年 1月 TRANSACTIONS OF THE CHINA WELDING INSTITUTION January 2006

CO_2激光焊接的同轴检测与熔透控制

III. 板厚变化时熔透状态同轴光信号分析

张旭东, 陈武柱, 刘 春, 国 静
(清华大学 机械工程系, 北京 100084)

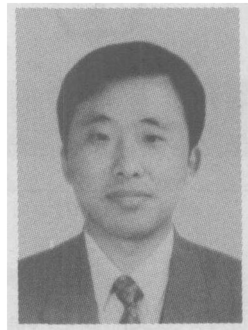

张旭东

摘 要: 利用 CO_2激光深熔焊等离子体光信号的同轴检测系统, 对工件板厚变化时激光焊接熔透状态的同轴光信号进行了时域和频域分析。结果表明, "适度熔透"状态时对应的等离子体同轴光信号强度最大, "未熔透"与"过熔透"状态对应的信号强度均小于"适度熔透"; 频域分析表明, "适度熔透"状态对应的 2~6 kHz段频谱重心最小。

关键词: 激光焊接; 同轴检测; 熔透; 斜板
中图分类号: TG456. 7 文献标识码: A 文章编号: 0253-360X(2006)01-13-04

0 序 言

在大多数激光焊接中, 焊缝的熔透状态是衡量焊接成形质量最重要的指标之一, 获得均匀适度熔透是保证焊接质量的前提。在以小孔效应为特征的激光深熔焊中, 根据小孔及熔池穿透工件的不同程度可将激光焊的熔透状态分为未熔透、仅熔池透(小孔未穿透工件)、适度熔透(小孔刚好穿透工件)和过熔透(小孔穿透工件, 但焊缝凹陷严重)四种熔透状态。其中适度熔透是最为理想的熔透状态[1~3], 也是激光焊接熔透控制的基准。

激光焊接过程中可能引起熔透状态波动的因素主要有两方面。一方面, 激光功率、焊接速度或焦点位置等工艺参数在焊接过程中可能出现的波动是引起熔透状态变化的主要原因。作者曾对激光功率和焊接速度变化时熔透状态的变化规律及相应的等离子体光信号特征进行了研究[1,2]。另一方面, 在稳定的焊接工艺条件下, 待焊工件的某些特性, 如板厚不均匀或焊接变形等也会导致熔透状态的波动。如何在这种情况下实时监测熔透状态的变化并通过调整焊接工艺参数来保证均匀适度熔透, 也是激光焊接熔透控制的重要内容。文献[4]通过在工件背面安装光电传感器对熔透状态进行检测, 并通过调整激光功率实现了搭接焊(板厚突变)时的均匀熔透控制。这种背面安装传感器的方法工业应用受到限制, 且对板厚逐渐变化的情况没有考虑。其他一些学者也在激光熔透状态的检测与控制方面进行了大量的研究工作[5~8], 但没有对板厚变化时熔透状态的变化规律及其检测信号进行研究, 对熔透信号的频域分析也做得较少。

作者利用研制的 CO_2激光焊接的同轴光学检测系统进行了斜板(板厚连续变化)激光焊接试验, 研究了不同熔透状态下同轴光辐射信号的时域和频域特征。

1 试验方法

图 1所示是 CO_2激光焊接同轴检测系统组成示意图, 该系统的核心是一个可以允许 10.6 mm 波长的 CO_2激光透过, 对由焊接区域产生的光辐射(主要是焊接等离子体, 也包括熔池)则几乎全部反射到分光镜。CO_2激光经平面反射镜入射到分光镜上, 经分光镜后再经一个焦距为 127 mm、直径为 40 mm的 ZnSe透镜聚焦后作用在工件表面。焊接过程中由等离子体或熔池发出的光辐射经透镜后再照射到分光镜上, 由于分光镜只允许远红外波段光通过, 这部分由焊接区域产生的光辐射被分光镜反射到光电传感器中, 光电传感器产生的信号通过处理单元输入到计算机进行处理。该系统的采样频率为 50 kHz。

图 2所示是激光焊接试验使用的低碳钢板试样尺寸, 板厚由 1 mm 连续变化至 3 mm。激光器使用 3 kW CO_2快轴流激光器, 连续工作模式, 光束模式为 TEM 00+01*。焊接时分别由板薄一侧向板厚

收稿日期: 2004-10-08
基金项目: 国家自然科学基金资助项目(50175061)

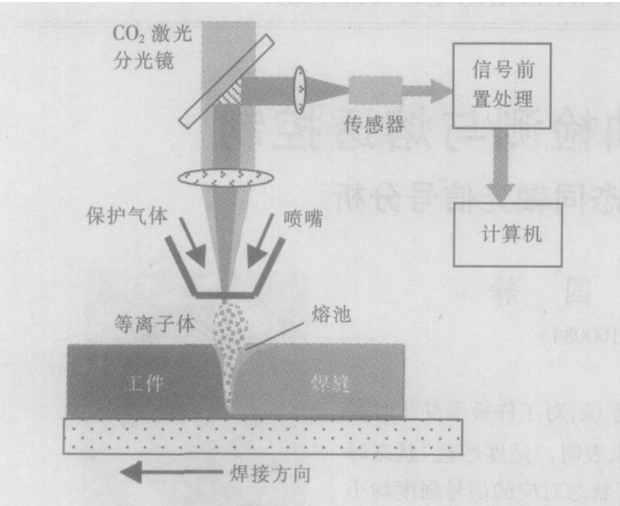

图 1 CO_2 激光焊接同轴光检测装置示意图

Fig. 1 Experimental setup of coaxial monitoring system for CO_2 laser welding

一侧或反方向焊接, 焊接过程中焦点位置在工件表面并保持不变。焊接时使用氩气作为保护气体。

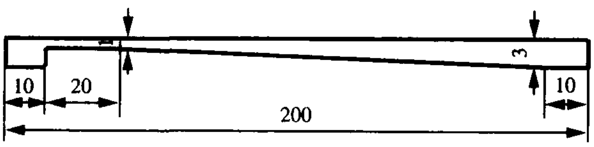

图 2 焊接试验中使用的斜板试样尺寸

Fig. 2 Sizes of workpieces used in welding experiments

2 试验结果和分析

2.1 斜板焊接时的信号时域分析

图 3所示为激光功率 $P=1\ 500$ W, 焊接速度 $v=0.8$ m/min, 焊接方向从板厚到板薄, 等离子体光检测信号强度的变化曲线 (采样频率 50 kHz)。可以看出, 正常开始焊接后, 随着板厚的变薄, 信号初始段 (*AB*)基本保持不变; 随着板厚的继续变薄, 信号 *BC*段开始上升, 达到最高值 (对应 *C*点)之后, 信号进入 *CD*段并开始下降, *DE*段代表焊接已经进行到斜板最后一段 (固定板厚 1 mm)。在图中标识出信号开始爬升 (图中 *B* 点)和达到最大值 (图中 *C* 点)的位置。图 4所示为对应图 3中 *B*点和 *C*点的焊缝横断面照片。可以看出, 图 4a的焊缝成形呈倒三角形, 属于 "仅熔池透 ", 而图 4b属于适度熔透状态, 焊缝呈双曲线形。

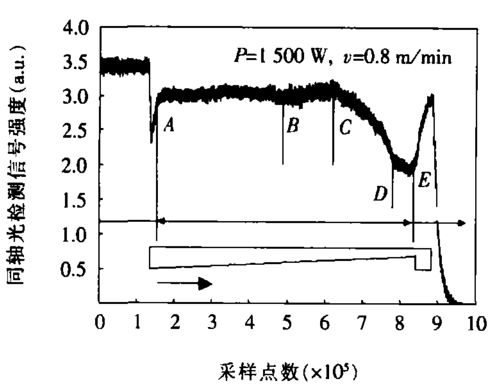

图 3 斜板激光焊接时等离子体光信号变化

Fig. 3 Plasma signal during laser welding of oblique plate

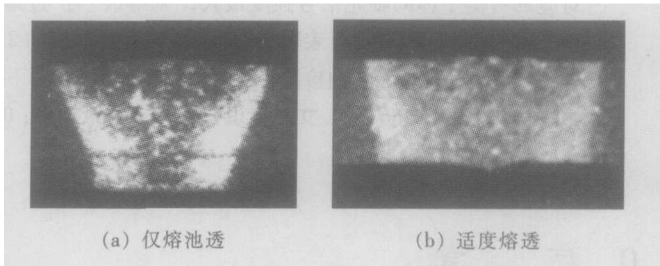

图 4 对应图 3中 *B*点和 *C*点的焊缝断面照片

Fig. 4 Weld cross sections at *B* and *C* positions in Fig. 3

图 5所示是激光功率 1 500 W, 焊接速度 0.8 m/min, 焊接方向从板薄到板厚时等离子体光信号的变化。斜板焊接方向从板薄到板厚的时候, 信号变化趋势正好与焊接方向从板厚到板薄对应信号变化趋势相反。从图中可以看出, 信号 *ED*段, 对应板厚固定为 1 mm段, 同轴光检测信号基本保持在一个较小的值上, 随着板厚的增加, *DC*段信号逐渐增加并达到最大, 然后 *CB*段信号开始下降, 最后在 *BA*段达到一个稳定值。在图中标注了信号达到最高点位置 *C*点和达到最高点后下降到稳定值的位

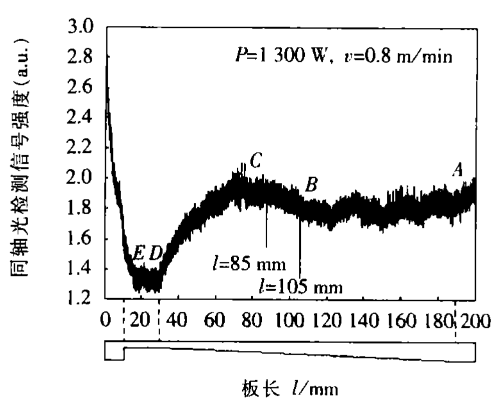

图 5 斜板激光焊接时等离子体光信号变化

Fig. 5 Signal variation with workpiece thickness

置 *B* 点。图 6所示为对应图 5中 *C* 点和 *B* 点的焊缝横断面照片。可以看出，图 6a的焊缝成形属于适度熔透状态，焊缝呈双曲线形，而图 6b的焊缝断面则呈倒三角形，属于"仅熔池透"。

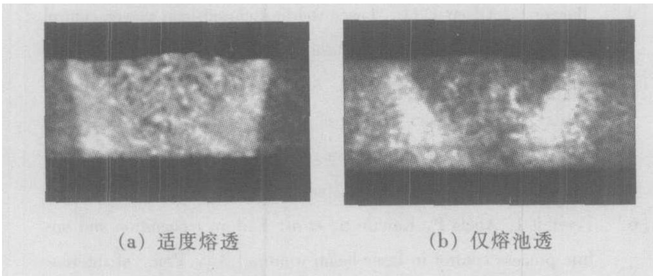

图 6　对应图 5中 *C* 点和 *B* 点的焊缝断面照片

Fig. 6　Weld cross sections at *C* and *B* positions in Fig. 5

图 7所示为固定的焊接速度 0.8 m/min，激光功率分别为 1 300W、1 500W 和 1 600W，焊接方向从板厚到板薄，对采样信号进行 1 000点平均后所对应的同轴光检测信号强度曲线，横坐标为试板长度。在图中以两端带箭头的竖线标注出了每条曲线的开始爬升点和最高点。经与焊缝成形对照，结果与图 3一样，当板从厚逐渐变薄的时候，同轴等离子体光检测信号在不透段均保持一稳定值，在出现熔池透的时候，检测信号开始爬升，出现"适度熔透（小孔穿透）"的时候，检测信号达到最大，此后，随着板厚继续变极薄，光信号开始下降。

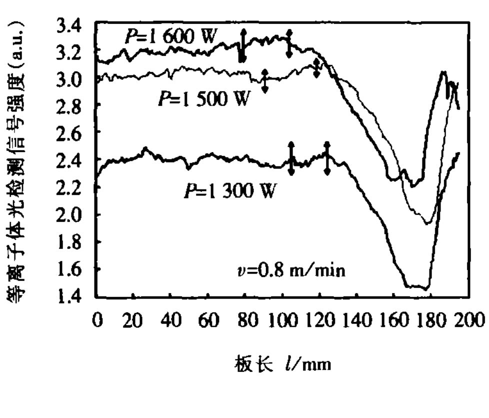

图 7　不同激光功率下斜板焊接的信号变化

Fig. 7　Signal variation with thickness under different laser powers

2.2　斜板焊接时的信号频域分析

在对激光焊接等离子体光信号进行频谱分析时，如果采用常用的周期图法短时傅里叶变化很难定量分析不同熔透状态下的信号特征，特别是不可能作为识别适度熔透的准确判据[2]。为此，作者在对平板焊接时的等离子体光信号进行频域分析时，提出了频谱重心的概念并以此来反映指定频谱段的频谱强度的性质。

频谱重心是指以某一频段频谱图形的重心所对应的频率坐标作为衡量频谱的定量指标，其数学表达式为

$$FreqG(i)=\frac{\sum_{f=f_{low}}^{f_{up}} f\times Power(i,f)}{\sum_{f=f_{low}}^{f_{up}} f\times Power(i,f)},$$

式中：$FreqG(i)$为频谱重心；f为频率；i为分段编号；f_{low}为统计频谱段的下限频率；f_{up}为统计频谱段的上限频率；$Power(i,f)$为第 i分段功率谱中频率 f所对应的功率谱强度。

为了反映频谱重心随时间的变化，对等离子体同轴光检测信号做带重叠的短时傅里叶分析，使用 AR（auto regressive）模型进行功率谱估计，并使用 Burg算法计算模型参数，然后再计算各分段的频谱重心。图 8所示为从斜板板厚一侧开始焊接时对检测信号（如图 3所示）进行短时傅里叶分析计算得到的 2～6 kHz段频谱重心随着时间变化的曲线。由图可见，当等离子体时域信号开始上升（即图 3中的 *BC* 段）时，对应焊缝状态由"仅熔池透"向"适度熔透（小孔穿透）"状态转变，此时 2～6 kHz段的频谱重心开始下降；当时域信号上升到最大值（图 3中 *C*点），对应的焊缝为适度熔透状态，此时 2～6 kHz段的频谱重心则降低至最低点；随着板厚继续变薄，当时域信号开始下降（图 3中 *CD* 段）时，对应的焊缝从适度熔透转变到过熔透状态，此时 2～6 kHz段的频谱重心则开始上升。

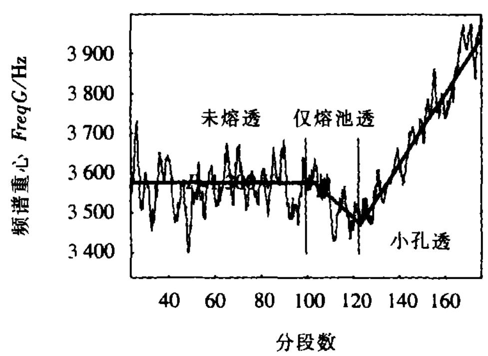

图 8　短时傅里叶分析中使用 AR模型估计功率谱并计算得到的频谱重心

Fig. 8　Barycenter of frequency spectrum of plasma signal obtained by using AR model

以上结果表明，斜板焊接时对应适度熔透状态的 2～6 kHz段的频谱重心最低，即适度熔透时同轴

光信号的频谱偏向低频。

3 结 论

(1)焊接热输入固定条件下,当板厚连续变化引起激光焊接熔透状态变化时,"适度熔透"对应同轴光时域信号强度的最大值,未熔透和"过熔透"对应的信号强度均低于"适度熔透"。

(2)当采用频谱重心定量表示熔透状态的等离子体光信号频谱特征时,板厚连续变化引起的熔透状态对应不同的频谱中心,其中适度熔透时 2~6 kHz段频谱重心最低(偏向低频)。

参考文献:

[1] Zhang Xudong, Chen Wuzhu, Liu Chun, et al. Coaxial monitoring and penetretion control in CO_2 laser welding(Ⅰ)——Penetration status characteristics and coaxial monitoring[J]. Transactions of the China Welding Institution, 2004, 25(1): 1-4.
张旭东, 陈武柱, 刘 春, 等. CO_2激光焊接的同轴光检测与熔透控制——Ⅰ. 熔透状态特性及其同轴检测[J]. 焊接学报, 2004, 25(4): 1-4.

[2] Zhang Xudong, Chen Wuzhu, Liu Chun, et al. Coaxial monitoring and penetration control in CO_2 laser welding(Ⅱ)——Frequency-field characteristics of coaxial optical signals[J]. Transactions of the China Welding Institution, 2004, 25(5): 25-28, 32.
张旭东, 陈武柱, 刘 春, 等. CO_2激光焊接的同轴光检测与熔透控制——Ⅱ. 熔透状态同轴光信号的频域分析[J]. 焊接学报, 2004, 25(5): 25-28, 32.

[3] 刘 春. CO_2激光深熔焊熔透同轴检测与控制的研究[D]. 北京: 清华大学, 2003.

[4] Bagger C, Olsen F O. Laser welding closed-loop power control[J]. Journal of Laser Applications, 2003, 15(1): 19-24.

[5] Sjoerd Postma, Aarts Ronald G K M, Johan Meijer, et al. Penetration control in laser welding of sheet metal using optical sensors[A]. Proc. of international congress on applications of laser and electro-optics2001[C]. Jacksonville, 2001.

[6] Petereit J, Abels P, Kaierle S, et al. Failure recognition and on-line process control in laser beam welding[A]. Proc. of international congress on applications of laser and electro-optics 2002[C]. Scottsdale, Arizona, USA, 2002.

[7] Isamu Miyamoto, Kiyokazu Mori. Development of in-process monitoring system for laser welding[A]. Proc. international congress on applications of laser and electro-optics 95[C]. San Diego, California, USA, 1995. 759-767.

[8] Gu Hongping, Duley W W. Discrete signal components in optical emission during keyhole welding[A]. Section G-international congress on applications of laser and electro-optics 97[C]. San Diego, California, USA, 1997. 40-46.

作者简介: 张旭东, 男, 1969年 9月出生, 工学博士, 副教授。主要研究方向为激光加工过程监测与控制、激光焊接技术等, 发表论文60余篇。

Email: xdzhang@tsinghua.edu.cn

[上接第 12页]

参考文献:

[1] Jaidi J, Dutta P. Three-dimensional turbulent weld pool convection in gas metal arc welding process[J]. Science and Technology of Welding and Joining, 2004, 9(5): 407-414.

[2] Kim I S, Basu A. A mathematical model of heat transfer and fluid flow in the gas metal arc welding process[J]. Journal of Materials Processing Technology, 1998, 77(5): 17-24.

[3] Dong Honggang, Gao Hongming, Wu Lin. Nunerical simulation of heat transfer based on PHOENICS during stationary palsma arc welding process[J]. Transactions of the China Welding Institution, 2002, 23(4): 24-26, 30.
董红刚, 高洪明, 吴 林. 固定电弧等离子弧焊接热传导的数值计算[J]. 焊接学报, 2002, 23(4): 24-26, 30.

[4] 赵玉珍. 焊接熔池的流体动力学行为及凝固组织模拟[D]. 北京: 北京工业大学, 2004.

[5] 董 平, 陈裕泽, 邹觉生, 等. 铍环激光束钎焊过程的数值模拟[J]. 金属学报, 2002, 38(8): 881-884.

[6] Dong Zhibo, Wei Yanhong, Liu Renpei, et al. Three dimensional numerical simulation of welding temperature fields in stainless steel[J]. China Welding, 2004, 23(1): 11-15.

[7] Kwon Y D, Choi W K, Kwon H W, et al. Effect of groove shape of ultra thick box-column with center segregation under high heat input for corner welding[J]. Key Engineering Materials, 2004, 261-263(1): 387-392.

[8] Goldak J. A new finite element model for welding heat sources[J]. Metallurgical Transactions B, 1984, 15B(2): 587-600.

作者简介: 徐艳利, 女, 1980年出生, 博士研究生。主要从事焊接过程流场温度场及热影响区晶粒长大三维组织模拟研究工作, 发表论文 1篇。

Email: xuyanli@hit.edu.cn

MAIN TOPICS, ABSTRACTS & KEY WORDS

A PZT driver signal acquisition and analysis system for ultrasonic wire bonding WANG Fu-liang HAN Lei ZHONG Jue (College of Mechanical and Electronical Engineering Central South University Changsha 410083 China). p1 – 4

Abstract According to the circuit of ultrasonic wire bonding experiment platform, a piezoelectric transducer (PZT) driver signal acquisition circuit was designed Then a signal acquisition and analysis system was designed with LabView and Matlab From the characteristics of the PZT voltage and current driver signals the methods were introduced in this system to calculate instant frequency virtual value curve and phase difference between them. Therefore some rules of the instant frequency and phase difference during the bonding process were obtained And extracting method of the characteristic points (for curve division) was also introduced based on the virtual value curve characteristics With the driver signals of 1 000 experiments the position stability of characteristic points was analyzed which was very important for bonding mechanism research. The experiment results showed that the system is stable and reliable and it can be used to acquire and analyze the PZT driver signal effectively.

Key words ultrasonic wire bonding PZT driver signal; signal acquisition and analysis system

Interface structure and bonding strength of brazed joint of TiC cermet/steel FENG Ji-cai JING Xiang-meng ZHANG Li-xia LIU Hong (National Key Laboratory of Advanced Welding Production Technology Harbin Institute of Technology Harbin 150001 China). p5 – 8

Abstract The vacuum brazing of TiC cermet (synthesized by SHS) to medium carbon steel was carried out with BAg45CuZn brazing filler metal and the interface structure and shear strength of the joints were also investigated by means of SEM, EPMA and XRD. The experimental results showed that the bonding of TiC cermet to medium steel can be performed with BAg45CuZn filler metal The interface structure of the joint is TiC cermet/(Cu, Ni) /Ag(s s) + Cu(s s) /(Cu, Ni) /(Cu Ni) + (Fe Ni) /medium carbon steel The maximum shear strength of the joint brazed at 850 ℃ for 10 min is up to 121 MPa at room temperature

Keywords TiC cermet steel vacuum brazing interface structure bonding strength

Comparison of GTAW temperature field of stainless steel simulated by different software packages XU Yan-li WEI Yan-hong DONG Zhi-bo ZHANG Yu-lin (State Key Laboratory of Advanced Welding Production Technology Harbin Institute of Technology Harbin 150001 China). p9 – 12 16

Abstract Two kinds of software packages were introduced and compared about their functions and characteristics The simulated results of the temperature field of stainless steel SUS310 in GTAW process showed that pre data treatment and post data treatment of MARC are more powerful than those of PHOENICS so it is easy for users to input the boundary conditions and get the results in MARC. But in PHOENICS the interfaces to the other software packages are provided for the post data treatment and the results can be operated easily in this way There is some difference between the results simulated by two software packages as the solvers are not the same. In MARC there are several integral points used to solve the results in every grid while in PHOENICS the staggered grid technique is used Simulated results of the two software packages show that the highest temperature calculated with MARC is 600 ℃ higher than that with PHOENICS

Key words temperature field GTAW; MARC; PHOENICS

Coaxial monitoring and penetration control in CO_2 laser welding (3) Relationship between optical signal and penetration statuses for oblique plate welding ZHANG Xu-dong CHEN Wu-zhu LIU Chun GUO Jing (Department of Mechanical Engineering Tsinghua University Beijing 100084 China). p13 – 16

Abstract Using a coaxial monitoring system for detecting the optical emission in CO_2 laser beam welding the time field and frequency field characteristics of the coaxial optical signals under different penetration statuses for welding of oblique plates were studied in this paper The experimental results showed that under constant laser power and welding speed the signal intensity varied with varying thickness and the signal intensity was maximum at the "moderate full penetration". In frequency field the barycenter of frequency spectrum (FBC) of 2 – 6 kHz range was minimum at the "moderate full penetration".

Key words laser welding coaxial monitoring penetration; oblique plate

Engineering critical assessment used for welded pipeline based on BS 7910 DENG Cai-yan[1], ZHANG Yu-feng[1], HUO Li-xing[1], BAI Bing-ren[2], LI Xiao-wei[2], CAO Jun[2] (1. School of Material Science and Engineering Tianjin University Tianjin 300072 China; 2. Offshore Oil Engineering Co. LTD Tianjin 300452 China). p17 – 20 25

Abstract British standard 7910 was applied to engineering critical assessment for welded joints of the API5LX56 pipeline steel with surface flaw at the weld toe. The failure assessment diagrams were derived from the tensile test results In accordance with the BS 7448 Part 4 frac